



**HAL**  
open science

## The X-TRACK/ALES multi-mission processing system: New advances in altimetry towards the coast

Florence Birol, Fabien Léger, Marcello Passaro, Anny Cazenave, Fernando Niño, Francisco M. Calafat, Andrew Shaw, Jean-François Legeais, Yvan Gouzenes, Christian Schwatke, et al.

### ► To cite this version:

Florence Birol, Fabien Léger, Marcello Passaro, Anny Cazenave, Fernando Niño, et al.. The X-TRACK/ALES multi-mission processing system: New advances in altimetry towards the coast. *Advances in Space Research*, 2021, 67, pp.2398-2415. 10.1016/j.asr.2021.01.049 . insu-03671350

**HAL Id: insu-03671350**

**<https://insu.hal.science/insu-03671350v1>**

Submitted on 22 Mar 2023

**HAL** is a multi-disciplinary open access archive for the deposit and dissemination of scientific research documents, whether they are published or not. The documents may come from teaching and research institutions in France or abroad, or from public or private research centers.

L'archive ouverte pluridisciplinaire **HAL**, est destinée au dépôt et à la diffusion de documents scientifiques de niveau recherche, publiés ou non, émanant des établissements d'enseignement et de recherche français ou étrangers, des laboratoires publics ou privés.



Distributed under a Creative Commons Attribution - NonCommercial 4.0 International License

## **The X-TRACK/ALES multi-mission processing system: new advances in altimetry towards the coast**

Florence Birol<sup>1</sup>, Fabien Léger<sup>1</sup>, Marcello Passaro<sup>2</sup>, Anny Cazenave<sup>1,3</sup>, Fernando Niño<sup>1</sup>, Francisco M. Calafat<sup>4</sup>, Andrew Shaw<sup>5</sup>, Jean-François Legeais<sup>6</sup>, Yvan Gouzenes<sup>1</sup>, Christian Schwatke<sup>2</sup> and Jérôme Benveniste<sup>7</sup>

<sup>1</sup> *LEGOS, University of Toulouse, IRD, CNES, CNRS, UPS, Toulouse, France*

<sup>2</sup> *TUM, Munich, Germany*

<sup>3</sup> *ISSI, Bern, Switzerland*

<sup>4</sup> *NOC, Liverpool, UK*

<sup>5</sup> *SKYMAT, Southampton, UK*

<sup>6</sup> *Collecte Localisation Satellites (CLS), Toulouse, France*

<sup>7</sup> *European Space Agency (ESA-ESRIN), Frascati, Italy*

**Corresponding Author:** Florence Birol

e-mail: [Florence.Birol@legos.obs-mip.fr](mailto:Florence.Birol@legos.obs-mip.fr)

tel: +33561332924

Submitted to *Advances in Space Research*, 11 September 2020

Revised, 13 November 2020

**Keywords:** Satellite Altimetry, Sea Level, Coastal Ocean

## **Abstract**

In the context of the ESA Climate Change Initiative project, a new coastal sea level altimetry product has been developed in order to support advances in coastal sea level variability studies. Measurements from Jason-1,2&3 missions have been retracked with the Adaptive Leading Edge Subwaveform (ALES) Retracker and then ingested in the X-TRACK software with the best possible set of altimetry corrections. These two coastal altimetry processing approaches, previously successfully validated and applied to coastal sea level research, are combined here for the first time in order to derive a 16-year-long (June 2002 to May 2018), high-resolution (20-Hz), along-track sea level dataset in six regions: Northeast Atlantic, Mediterranean Sea, West Africa, North Indian Ocean, Southeast Asia and Australia. The study demonstrates that this new coastal sea level product called X-TRACK/ALES is able to extend the spatial coverage of sea level altimetry data ~3.5 km in the land direction, when compared to the X-TRACK 1-Hz dataset. We also observe a large improvement in coastal sea level data availability from Jason-1 to Jason-3, with data at 3.6 km, 1.9 km and 0.9 km to the coast on average, for Jason-1, Jason-2 and Jason-3, respectively. When combining measurements from Jason-1 to Jason-3, we reach a distance of 1.2-4 km to the coast. When compared to tide gauge data, the accuracy of the new altimetry near-shore sea level estimations also improves. In terms of correlations with a large set of independent tide gauge observations selected in the six regions, we obtain an average value of 0.77. We also show that it is now possible to derive from the X-TRACK/ALES product an estimation of the ocean current variability up to 5 km to the coast. This new altimetry dataset, freely available, will provide a valuable contribution of altimetry in coastal marine research community.

## 1. Introduction

Since the early 1990s, several high-precision altimeter satellites routinely observe the ocean surface topography, resulting in a more than 25-year-long record of nearly-global sea level data. These observations have greatly improved our knowledge of the open ocean and are now an essential component of many operational marine systems. But in near-shore regions, satellite altimetry encounters different important issues (e.g. 30-50 km from the coast, see *Vignudelli et al., 2011* for a review), that makes it difficult to derive accurate geophysical data in coastal environments.

Firstly, in the coastal band of a few kilometers wide (corresponding to the altimeter footprint size), the radar echo interacts with the nearby land surface, leading to complex waveforms, that furthermore depend on the characteristics of both the coast (e.g. direction, topography, bathymetry, nature of the land surface, ...) and the altimeter instrument. These coastal waveforms are then difficult to interpret (*Gommenginger et al., 2011, Xu et al., 2018*). Another difficulty is related to the geophysical, environmental corrections that need to be applied to the altimeter measurements (e.g. wet troposphere, ionosphere, sea state bias, inverse barometer, high frequency wind effect and tides) and that often become inaccurate close to the coast (e.g. *Andersen and Scharroo, 2011*). The traditional use of altimetry data in the coastal ocean is also further complicated by the fact that their spatial and temporal distribution does not fully cover the scales of the near-shore ocean processes.

The fundamental importance of satellite altimetry in many oceanographic fields, and its potential for the quasi-global monitoring of coastal sea levels changes induced by ongoing climate change in particular (*Cipollini et al., 2017; Marcos et al., 2019*), have motivated the development of coastal altimetry studies. Since the 2000s, several projects (e.g. PISTACH, *Mercier et al., 2010*; PEACHI, *Valladeau et al., 2015*; COASTALT, *Vignudelli et al., 2009*;

X-TRACK, *Biol et al.*, 2017; e-Surge, <http://www.storm-surge.info/project>; ...) have been designed with the objective to exploit altimetry information with a better spatial resolution, as close as possible to the coastline. Algorithms have been developed to classify and/or retrack altimetry measurements in order to improve the retrieval of sea level parameters from coastal waveforms (*Mercier et al.*, 2010; *Passaro et al.*, 2014; *Peng and Deng*, 2018). Significant improvements have been also achieved in altimeter corrections (e.g. wet troposphere and ocean tide corrections, sea state bias), allowing one to obtain more accurate altimetry-derived coastal sea level data (*Fernandes et al.*, 2015; *Carrere et al.*, 2016; *Passaro et al.*, 2018). In parallel, innovations in radar techniques (synthetic aperture radar mode, on Cryosat-2, Sentinel-3A & 3B, and Ka-band altimetry on SARAL/AltiKa) have resulted in increased observational capabilities of coastal ocean processes (*Verron et al.*, 2018; *Vignudelli et al.*, 2019). Several studies have dealt with the coastal altimetry processing strategy and quality assessment of the resulting data (*Vignudelli et al.*, 2005; *Jebri et al.*, 2016; *Dinardo et al.*, 2018). Finally, the availability of new experimental coastal altimetry products (see <http://www.coastalt.eu/> for an updated table) has allowed researchers to demonstrate their unique value in coastal applications (see for example: *Troupin et al.*, 2015; *Vignudelli et al.*, 2019; *Gómez-Enri et al.*, 2019).

Today, coastal altimetry algorithms and methodological techniques are mature enough for the definition and delivery of a consistent and homogeneous long-term sea level product (e.g. addressing as much as altimetric missions as possible). It is clearly a critical need for sea level research in the coastal zone (*Benveniste et al.*, 2019). During the past decade, the sea level project of the European Space Agency (ESA) Climate Change Initiative (SL\_cci, [www.esa-sealevel-cci.org/](http://www.esa-sealevel-cci.org/)) has focused on producing a stable and homogeneous sea level Essential Climate Variable (ECV) product. This has led to an altimeter multi-mission monthly gridded product over the global ocean (*Ablain et al.*, 2015; 2017; *Legeais et al.*, 2018). In

2018, the extension phase of the activities (SL\_cci+) has been launched in order to address the issues identified in the coastal zone (e.g. 0-50 km coastal band) with a new multi-mission sea level altimetry product in selected regions (Fig. 2).

The aim of this paper is to present the coastal along-track altimetry product developed in the context of the SL\_cci+ project and to show how it will support advances in coastal sea level variability studies. It is organized as follows: The data processing and the product are described in Section 2. The quality of the corresponding dataset and its observational capability, in comparison to previous products, are assessed in Section 3. A case study is provided in Section 4. Finally, Section 5 summarizes main results and gives some perspectives.

## **2. Data processing and product description**

The SL\_cci+ project aims to take advantage of the progress made in previous studies in terms of coastal altimetry processing techniques, in order to generate the best possible regional multi-mission product dedicated to near-shore sea level research.

### **2.1 Data processing**

All the experimental coastal altimetry products already available differ in their waveform retracking and processing approach, geophysical corrections used, along-track resolution, and coverage in terms of missions, time period and regions. Today, one of the most widely used is the called X-TRACK product developed at the LEGOS laboratory and distributed by the AVISO+ operational centre (<https://www.aviso.altimetry.fr/index.php?id=3047>, [https://doi.org/10.6096/CTOH\\_X-TRACK\\_2017\\_02](https://doi.org/10.6096/CTOH_X-TRACK_2017_02)). It is a 1-Hz along-track product (i.e. with a resolution of 6-7 km in the along-track direction) that covers all the coastal oceans with the reprocessing of different altimetry missions (Topex/Poseidon, Geosat Follow-on, Envisat,

Jason-1,2,3, SARAL and Sentinel-3A), It is based on an editing and post-processing strategy defined to optimize the completeness and the accuracy of the sea surface height (SSH) derived from satellite altimetry in coastal ocean areas. The X-TRACK system is described in detail in *Roblou et al. (2011)* and *Birol et al. (2017)*. Here we only provide in Figure 1 an illustration of the impact of the X-TRACK procedure on the retrieval of coastal sea level variations from altimetry. The differences between the sea level anomalies (SLA) obtained along Jason 2 track 9 in the Mediterranean Sea before and after the X-TRACK algorithm are clearly observed, with much less abrupt changes in SLA in the X-TRACK solution. Figure 1 (left) also indicates that the corresponding signal variance is significantly lower near the coast, corresponding to a reduction of the geophysical corrections uncertainties with X-TRACK. This product is based on the standard open-ocean altimeter waveform retracker (called MLE4) and provides sea level anomaly time series up to 5-10 km to the coast (*Birol et al., 2017*).

The Adaptive Leading-Edge Subwaveform (ALES) retracker has been designed to take into account the interferences often observed in coastal altimeter echoes (*Passaro et al., 2014*). These interferences are due to the presence of land or inhomogeneities in the surface illuminated by the radar and are usually confined in the trailing edge of the returned echo (waveform). ALES maintains a better accuracy of sea level estimates derived from altimetry waveforms collected in the coastal zone, in comparison to standard open-ocean retrackers. The retracker is based on a first estimation of the significant wave height (SWH) limited to the leading edge portion of the waveform, which contains the geophysical information necessary to estimate the distance between the satellite and the ocean surface (range). Subsequently, the width of the subwaveform is adapted based on the SWH and a second fitting is performed in order to guarantee higher precision of the measurement. Full details of the ALES retracking algorithm are given in *Passaro et al. (2014)*. The benefit of the ALES

retracking procedure in the open ocean has been also observed in the analysis of its spectral properties. The sea level estimations based on ALES present a reduced noise at the mesoscale, improving the representation of the oceanic scales of variability between 50 and 10 km wavelengths (*Smith et al.*, 2017).

The efficiency of these two different approaches (e.g. ALES and X-TRACK) to improve both the quantity and the quality of coastal altimetry sea level data has been demonstrated in many different studies (for example: *Birol et al.*, 2010; *Passaro et al.*, 2015; *Piccioni et al.*, 2018). In the context of SL\_cci+ project, in order to improve the observing capability of coastal processes, X-TRACK has been first extended to the processing of high-rate altimetry measurements (20-Hz in the case of Jason missions: a resolution of ~0.3 km in the along-track direction) instead of the previous 1-Hz data. It has then been adapted to the ingestion of the data outputs of the ALES retracker. In terms of altimetry corrections, except the pole tide and sea state bias (SSB), the altimeter standards defined in the ESA SL\_cci project for sea level estimates dedicated to climate studies were selected (*Quartly et al.*, 2017). The SSB correction is computed for every 20-Hz measurement applying the model developed by *Tran et al.* (2010) to the sea state retrievals of the ALES retracker. This approach has been demonstrated to improve the precision of the measurement by decreasing the variance of the SSH differences at crossover points by 10 to 20% depending on the region (*Passaro et al.*, 2018). The resulting new processing system is called X-TRACK/ALES.

The X-TRACK/ALES system reprocesses in delayed time the Geophysical Data Records (GDRs) provided by the space agencies for the different altimetry missions. Its inputs are listed in Table 1. The altimetry corrections account for atmospheric effects (wet and dry troposphere, ionosphere, inverse barometer), geophysical phenomena (ocean tides, high frequency atmospheric effects on the ocean) and the sea-surface state (electromagnetic sea-surface bias). Since, except the latter, they are provided at 1-Hz, they are recomputed at the

high-rate 20-Hz frequency through the interpolation/extrapolation methods described in *Biol et al.*, 2017. Corrected sea surface heights (SSHs) are then computed at 20 Hz along-track points using Equation 1. They are further projected onto fixed points along a nominal ground track and converted into Sea Level Anomalies (SLA) by subtracting a precise Mean Sea Surface (MSS) height using Equation 2.

$$\text{Corrected SSH} = \text{Orbit} - \text{Range} - \Sigma(\text{corrections}) \quad (1)$$

$$\text{SLA} = \text{Corrected SSH} - \text{MSS} \quad (2)$$

The MSS is computed at the fixed nominal points, by inversion of all the available corrected SSH data available along the repeated ground tracks of the altimetry mission considered. This procedure allows us to better solve the coastal MSS gradients than the use of a standard gridded MSS product and then to reduce the errors in coastal SLA data (*Vignudelli et al.*, 2005). More details on the MSS computation can be found in the X-TRACK/ALES Algorithm Theoretical Basis Document ([http://www.esa-sealevel-cci.org/webfm\\_send/628](http://www.esa-sealevel-cci.org/webfm_send/628)).

## 2.2 The X-TRACK/ALES SLA product

As X-TRACK, the X-TRACK/ALES reprocesses data on a regional basis. Figure 2 shows the regions which are currently being processed within the SL\_cci+ project: Northern Europe, Mediterranean Sea, Western Africa, North Indian Ocean, Southeast Asia and Australia.

In a first attempt, altimetry missions that share the same orbit (e.g., Jason1, Jason-2 and Jason-3) have been reprocessed in order to maximize the length of the resulting sea level time series. We consider Jason-1 data from January 2002 to January 2009 (259 cycles), Jason-2 data from July 2008 to September 2016 (303 cycles) and Jason-3 data from February 2016 to May 2018 (84 cycles). At this stage of the X-TRACK/ALES processing, for each Jason mission and each region, we obtain SLA time series at a near 10-day sampling (Jason orbital cycle) and with a spatial resolution of ~0.3 km along the tracks. The computation of a single

long-term multi-mission product requires the application of inter-mission biases (corresponding to instrument and corrections biases) in order to obtain stable sea level time-series. These biases are computed during the “calibration phases” between two consecutive missions, when both satellites fly on the same ground track with about one minute time lag, with the following method. For each region, we compute the difference in sea level observed by the two satellites at the same locations during the “calibration phase”. These differences are then first averaged over time, low-pass filtered in the along-track direction (with a 40-km cutoff frequency) and further averaged over  $1^{\circ} \times 1^{\circ}$  boxes. The corresponding smoothed  $1^{\circ} \times 1^{\circ}$  bias values are finally interpolated at the original 20-Hz along-track altimetry points and applied to the SLAs. Altimetry points located at less than 10 km from the coast, as well as points where more than 20% of data are missing in the time series are excluded from the computation because they contain more uncertainties (in the first case) or because the difference in the number of data samples between the two missions introduce errors in the inter-mission biases. The Jason-1/2 inter-mission bias is applied to Jason-2 SLAs first (at Jason-2 cycle 21), and then Jason-2/3 inter-mission bias to Jason-3 SLAs (at Jason-3 cycle 24). Note that this bias also absorbs the possible artefact introduced by a SSB correction estimated from SWH and sigma0 derived from different missions. It is worth mentioning that no orbit error reduction has been applied to the coastal sea level product. This is because such a correction based on differences between ascending and descending satellites tracks due to orbit errors needs to be computed globally. However, given the large-scale signature of the orbit error and the fact that the product is designed for climate applications, the impact of this correction is expected to be small. For each region, we finally obtain a single along-track multi-mission 20-Hz SLA product for the period from 15 January 2002 to 30 May 2018 (e.g. at the time of writing, for a total of 603 cycles). The corresponding XTRACK/ALES product, also called coastal SL\_cci+ product, is available through DOI: <https://doi.org/10.5270/esa->

sl\_cci-xtrack\_ales\_sla-200206\_201805-v1.1-202005 and more details can be found in the Product User Guide (currently v1.3, available at: <http://www.esa-sealevel-cci.org/PublicDocuments/technical>). Note that the temporal coverage of the product will be regularly extended in the future.

### **3. Performance and Validation**

A first version of the processing system described above has been successfully evaluated and validated in *Marti et al. (2019)* along the coasts of Western Africa (with Jason-1 & Jason-2 data). It has been further applied in *Gouzenes et al. (2020)* and *Coastal Sea Level Project Team (2020)* to estimate coastal sea level trends in different regions. Valid reprocessed sea level data were shown to be still available at less than 3 to 4 km to the coast, depending on the location, compared to 5 to 10 km in the standard X-TRACK product. In this section we first provide a quantitative evaluation of the impact of the combination of ALES and X-TRACK high-rate processing system on the coastal sea level data availability and quality (section 3.1). A regional comparison between X-TRACK/ALES and the 1-Hz X-TRACK coastal product distributed by AVISO+ is also performed. The quality of the new X-TRACK/ALES product is then assessed through a comparison with a large number of tide gauge (TG) observations (section 3.2).

#### **3.1 Respective gain inferred by the ALES retracker and the original high-rate sampling rate in coastal sea level data**

In order to first analyse the respective impact of using the original 20-Hz sampling altimeter measurements and of using the ALES retracking algorithm, a third SLA dataset called X-TRACK 20Hz is computed. It is derived with exactly the same procedure than the X-TRACK/ALES data, except that the altimeter range and SSB are extracted from the classical

MLE4 ocean retracker. In this section, only the three regions corresponding to the first phase of the SL\_cci+ project are considered: Northern Europe, Mediterranean Sea, Western Africa (Figure 2), for both Jason-1 and Jason-2. We use the along-track mono-mission SLA data (e.g. before the multi-mission combination described in section 2.2).

The relative performance of the different processing strategies is first evaluated in terms of coastal sea level data availability. For each dataset, we compute the percentage of defined SLA data obtained after X-TRACK or X-TRACK/ALES processing (relative to the total number of satellite cycles considered in the time series) for each altimetry point along all the Jason tracks crossing the three regions considered. Indeed, as shown for example in *Biol and Delebecque* (2014, see Figure 2) or in *Vignudelli et al.*, (2019, see Figure 4), this value decreases abruptly when approaching the coast but differs significantly from one altimeter to the other and/or from one processing strategy to the other. It is then a relevant metric to compare near-shore altimeter data performances. Moving away from the coast, for each track crossing the land surface, the distance of the first altimetry points where more than 80% of the SLA are defined is stored and used to compute regional boxplots of the distribution of the “distance to coast” values (in km), as a function of the mission and of the dataset (Figure 3). Finally, the regional median values of distances to the coast obtained in Figure 3 (indicated by the red lines) are summarized in Table 2, according to the altimeter mission, data set and region considered. For each region, the number of tracks considered is also indicated in this table.

In Figure 3, the positive impact on the near-shore data availability of using both the original 20-Hz sampling altimeter measurements and the ALES retracking algorithm in SLA data processing is obvious for all regions and for both Jason-1 and Jason-2. In all cases, the use of the original 20-Hz measurements significantly extends the coastal SLA data availability, relative to conventional 1-Hz data. This result was already shown by *Biol and*

*Delebecque* (2014) in the Northwestern Mediterranean Sea with a much lower sample of data. But here we observe that the ALES retracker systematically increases the number of defined coastal altimetry data. Examining in more details Figure 3 and Table 2 it appears that:

- For Jason 2, the data availability starts always to decrease closer to the coastline: 6.21 km on average for X-TRACK 1Hz (2.39 km for X-TRACK/ALES) against 7.46 km for Jason-1 (4.03 km for X-TRACK/ALES). It is explained by the better acquisition and tracking mode of Jason-2, resulting in less data loss in coastal zones (*Desjonquères et al.*, 2010).
- For Jason-1, 80% of SLA data are available on average at 7.46 km to the coast in X-TRACK 1Hz, against 4.79 km in X-TRACK 20Hz and 4.03 km when we combine ALES with the high rate X-TRACK processing. For Jason-2, these numbers fall to 6.21 km, 2.64 km and 2.39 km, respectively.
- Dataset statistics and data processing performance, vary significantly from one region to the other. The best statistics are observed in the Mediterranean Sea, with 80% of data available on average, at 3.31 km (1.19 km) to the coast for Jason-1 (Jason-2) when using X-TRACK/ALES. Off the Western African coasts, the best results are also observed with the same dataset but we obtain 4.84 km (3.38 km) to the coast for Jason-1 (Jason-2).

To summarize, by using the high rate (e.g. 20 Hz) altimetry measurements instead of 1-Hz data, we achieve an availability rate of 80% of defined SLA ~3 km shoreward along the ground track, and reach a distance of ~3-5 km to the coast on average. When combined with the ALES retracker, the extension increases to ~3.5 km, allowing one to reach a distance of 2.5-4 km to the coast on average. The next step is to assess whether this data gain is associated to coherent physical signals or to larger noise and coastal measurement errors.

First, the standard deviations (STD) of the SLA time series have also been calculated at each reference point along the different ground tracks for each region and satellite mission, using X-TRACK 1-Hz, X-TRACK 20-Hz and X-TRACK/ALES. Statistics have been computed only for time series for which the number of available SLA data is equal to or larger than 80% of the total number of cycles processed. For both Jason-1 and Jason-2, the statistics are averaged per region and are represented as a function of the distance to the coast (Figure 4). For clarity, we focus on the data that are less than 50 km from land. Note that, in the 0-5 km coastal band, statistics tend to be generally lower in the Western Africa region but they are computed from less sample data than in the other regions.

In Figure 4, X-TRACK 1-Hz shows lower standard deviation values than the other two datasets (on average, 2.6 cm lower than X-TRACK 20-Hz and 2.4 cm lower than X-TRACK/ALES), which was expected since 1-Hz altimeter data are derived from a 20-point boxcar average of the original 20-Hz measurements. This number is close to the one obtained in *Birol and Delebecque (2014)*, who also showed that by filtering the high-rate SLA data measurements with a low-pass filter, it is possible to obtain the same level of sea level accuracy as when using the 1-Hz SLA data, while retaining more data closer to the coast. This gain in coastal altimetry data is indeed also found in the present study (Figure 3 and Figure 4). In Figure 4, a change in STD curves is also observed 5-10 km from the coast, depending of the data set and the region. The near-shore STD values associated to 20-Hz data grow much faster when approaching the coast than the values associated to 1-Hz data. This change is systematic and much larger in all data sets if we use all the data available and not only the time series with 80% of SLA available (not shown), likely indicating the presence of inaccurate near-coastal altimeter measurements in the 20-Hz data that have not been discarded by the X-TRACK process. It shows that there is room to further improve the high-rate altimetry data processing. However, at distances shorter than ~10 km from the coast, this

increase in STD values is significantly lower in X-TRACK/ALES than in X-TRACK 20-Hz, especially for Jason-2 (Figure 4b).

Six tide gauge stations distributed at different coastal sites of the three regions have then been used to further evaluate the quality of the SLA datasets near the shore (Table 3). They have been chosen because of the length of their time series, the time span of data available, and because of their location (seeking to maximize the number of samples in the statistics and to minimize the distance between the tide gauge station and Jason SLA points). The data are provided by the SHOM (<https://data.shom.fr>) and by the University of Hawaii (<http://uhslc.soest.hawaii.edu/network/>). Note however that tide gauges and altimeter observations are not collocated and do not measure exactly the same sea level variations.

To make in situ sea level as consistent as possible with the altimeter SLA data, the tidal signals were removed from the hourly tide gauge observations (using harmonic analysis) and the same atmospheric correction was applied (see Table 1). Concurrent time series from tide gauges and altimetry SLA were finally obtained by removal of the mean sea level value computed over the same time period. For each tide gauge station, we consider the nearest altimetry points where more than 80% of data is available in the time series and we computed the root mean square of the differences (RMSD) and correlation coefficients between the in-situ and altimetry SLA time series, using X-TRACK 20Hz, X-TRACK 1-Hz and X-TRACK/ALES 20-Hz SLA time series. These statistics are summarized in Table 3.

Compared to 1-Hz data, the much higher level of noise in the 20-Hz altimeter data illustrated in Figure 4 results in significantly lower correlation and significantly higher RMSD values with independent tide gauge observation (Table 3). Based on the results of *Birol and Delebecque* (2014), we then filter out the noise in all SLA datasets with a low-pass Loess filter applied in the along-track direction. A cut-off frequency of 40 km has been chosen (corresponding to the frequency of the filtered version of the 1-Hz X-TRACK product). The

statistics computed from both the filtered 20-Hz and 1-Hz SLA now closely agree. When compared to the other altimetry solutions, the near-shore altimeter SLA processed with the X-TRACK/ALES system are in better agreement with the equivalent ground truth; we obtain lower RMSD values, larger correlation coefficients and data available closer to the coast (except for the Sète tide gauge for which the correlation decreases slightly). By spatially filtering the X-TRACK/ALES high-rate SLA measurements, we obtain a better level of sea level precision as we would using the X-TRACK 1-Hz altimeter data, while minimizing significantly the data gap in altimetry next to the coast.

### **3.2 General statistics of the X-TRACK/ALES SLA product and validation against tide gauge data**

We now recompute the median distance to the coast of the first point (in km) where more than 80% of the SLA data from the X-TRACK/ALES product is available, but considering the six regions and the three altimeter missions of the project, separately and combined. The results are provided in Table 4, according to the altimeter mission, and region considered. All the values are in a 0.5-5 km coastal band. On average, we obtain values of 3.6 km, 1.9 km and 0.9 km to the coast, for Jason-1, Jason-2 and Jason-3, respectively. This result confirms the clear improvement in the performances of nadir-pointing altimetry missions over coastal areas achieved during the last decade. Considering now the multi-mission dataset, we obtain a mean value of 2.9 km, indicating that the weaker performance of Jason-1 data may be a strong limitation for coastal studies that need long-term sea level data. Note also that for Jason-1 and Jason-2, the statistics obtained here considering six regions instead of only three in the previous section, are slightly lower: 3.6 km / 1.9 km for Jason-1 / Jason-2 instead of 4.03 km / 2.39 km. It is explained by the very good coastal data availability achieved in the Southeast Asia and Australia regions (especially for the Jason-2 and Jason-3 missions). More generally,

a significant spread is observed in the distance to coast data availability from one region to the other: from 1.7 to 4.7 km for Jason-1, from 1 to 3.4 km for Jason-2, from 0.5 to 1.3 km for Jason-3 and from 1.2 to 4 km for Jason-1,2,3 combined. It is probably due to the shoreline characteristics which differ from area to the other and impact the waveforms and corrections in a different way. This impact seems to significantly decrease in the most recent altimetry missions.

The X-TRACK/ALES sea level product has then been compared against tide gauge data in the six study regions. The tide gauge data used here consists of monthly mean values of sea level obtained from the Revised Local Reference data archive of the Permanent Service for Mean Sea Level (PSMSL) (<http://www.psmsl.org/>) (Holgate *et al.*, 2013). We select 78 stations in northwestern Europe, 48 in the Mediterranean Sea, 2 in Western Africa, 7 in the North Indian Ocean, 58 in southeast Asia, and 55 in Australia. To be consistent, the same atmospheric correction is applied to the altimetry data and to the tide gauge data (Table 1). The validation is conducted in terms of sea-level variability (detrended monthly time series of sea level with the annual and semi-annual cycles removed) over the period from January 2002 to May 2018. In designing the validation strategy, a number of points merit consideration.

First, it is important to recognize that while the tide gauge data from the PSMSL represent true monthly mean values, the along-track altimetry data consists of at most four measurements per month at any particular location. This difference in temporal sampling will manifest as differences in the sea level variability captured. Exploratory analysis of this issue (not shown here) indicates that this sampling effect is fairly small when using three or more altimetry SLA values per month. However, when using only one value per month, it can degrade the correlation between the two otherwise identical time series, on average, from 1 to 0.7. In addition to this, as mentioned in section 3.1, altimetry measurements are not taken at the tide gauge locations but at some ocean point nearby. The importance of the resulting

differences between the two types of data due to spatial separation will necessarily depend on the length scales of the sea-level signals around the tide gauges.

To minimize the impact of errors due to spatial separation on our validation and alleviate the issue of sampling uncertainty, we use here an approach that merges altimetry data from different tracks based on the sea-level length scales around the tide gauges. This approach involves estimating coherence length scales of sea level variability at each tide gauge by correlating the deseasoned and detrended sea-level from the tide gauge record with that from along-track altimetry, and then fitting a Matérn function with smoothing parameter  $\nu=5/2$  (*Rasmussen and Williams, 2006*) to the vector of correlations as a function of distance to the tide gauge. We chose a Matérn function because, on average, it provides the best fit to the data based on R-squared values. We also considered other correlation functions but the differences obtained were sufficiently small to conclude that our results are not sensitive to this choice. Length scales are computed separately for each track and so different tracks might have different length scales. Then, at each tide gauge, we merge the altimetry data from all tracks that fall within the estimated length scales into a monthly time series by averaging spatially along tracks and temporally (measurements corresponding to the same month) across tracks. We construct two types of altimetry timeseries at each tide gauge: 1) we merge all the altimetry data from all tracks that fall within the characteristic length scale into one single altimetry timeseries (this is our ‘best’ altimetric estimate); and 2) we bin and merge the altimetry data that fall within the length scale according to distances to the coast at intervals of one kilometre, thus generating one altimetry timeseries for each distance to the coast. Timeseries 2) enables us to assess the performance of the altimetry data as a function of distance to the coast. As part of the processing of the altimetry data, we remove values of SLAs beyond both 2 m and 3 standard deviations (over the period 2002-2018); this is the only editing of the altimetry data involving outlier rejection that we conduct here.

Using only altimetry data within a length scale from the tide gauge can reduce differences due to spatial separation. In addition, if more than one altimetry track falls within the estimated length scale, our approach allows us to compute monthly values based on many more than 4 values, reducing the effect of sampling uncertainty. For example, if two tracks fall within the length scale, we are able to compute monthly means using up to 8 values per month, and so on. In our case, altimetry monthly means are based on 9 or more values at 77% of the data stations (on average over the period 2002-2018). The length scales have an average value of 203 km (here the length scale is defined as the distance at which the correlation between the altimetry and tide gauge observations falls below 0.4), but they vary significantly across locations and regions (not shown). For example, along the western Australian coast and in the German Bight the length scales can be as large as 300 km or more, whereas along the European Atlantic coast and in the English Channel length scales of 160 km or less are common. As we will see later, regions with long length scales coincide with regions where there is a better agreement between the altimetry and tide gauge observations.

Before moving to the comparison in terms of deseasoned timeseries, we note that at many coastal locations the sea-level annual cycle is the most energetic signal outside the tidal frequency band and so a comparison between the altimetry and tide gauge data in terms of this cycle provides a first-order assessment of the data and might highlight the existence of gross errors. We find that, on average, differences in the amplitude of the annual cycle between the altimetry and tide gauge timeseries are only 17% of the value of the amplitude, indicating a very good match between the two types of measurements.

The correlation between detrended, deseasoned sea level from tide gauge records and satellite altimetry (the ‘best’ altimetric timeseries) is shown for the six study regions in Fig. 5. The correlations are fairly uniform across both tide gauge stations and regions with a mean value of  $\sim 0.77$ , indicating an overall good match between the two types of measurement.

While, in general, differences in correlation tend to be small across stations, a clear spatial structure is noticeable in some of the regions. This is most obvious along the Australian coastlines (Fig. 5F), where correlations are higher along the western coast compared to the eastern coast. This may be related to the differences in the length scales of sea-level signals, longer along western Australia (with an average value of 293 km as compared to 200 km along the eastern Australian coast). But the fact that the tracks go from sea to land in western Australia and from a mountainous region to sea along the eastern coast might also play a role in explaining the differing performance.

The correlations shown in Fig. 5 are based on altimetric timeseries that are formed by merging all the altimetry data that fall within a characteristic length scale at each tide gauge (what we call ‘best’ altimetry timeseries). However, we can further group the altimetry data in terms of distance to the coast as described earlier in this section and this can be used to obtain a measure of the closest location to the coast at which the altimeter performance remains high. At most locations the closest we can get to the coast before correlations start to drop is between 2 and 6 km, with a mean value of 4 km (not shown). There are very few locations where we can get closer than 1 km without seeing a substantial decrease in correlation between the tide gauge and altimetry data.

#### **4. Case study: the value of the X-TRACK/ALES sea level product in capturing coastal currents**

The X-TRACK/ALES coastal sea level product, which includes the most recent algorithm developments done in the coastal altimetry community, has been designed for estimating rates of coastal sea level change as close as possible to the coastlines. This is the objective of the ESA Climate Change Initiative coastal sea level project mentioned in the introductory part, with the ultimate goal of determining how coastal sea level change at the coast compares to

the open ocean sea level change. Preliminary results of coastal sea level trends over the 2002-2018 time span in the six regions mentioned above, based on the X-TRACK/ALES product are presented in another article (*The CCI Coastal Sea Level Team, 2020*; see also *Gouzenes et al., 2020*).

However, the X-TRACK/ALES sea level dataset described above can be used for other applications, in particular the study of the coastal ocean circulation. We briefly describe below a case study, focusing on the Northern Current (NC) located in the Northwestern Mediterranean Sea. This particular region has already been used several times to assess the information content of different SLA altimetry datasets with respect to near-shore currents (for example: *Birol and Niño, 2015*; *Carret et al., 2019*). The NC is a surface boundary current that flows cyclonically along the coasts of Italy, France and Spain (*Millot, 1991*); despite its narrow width (~20–50 km), altimetry datasets have the potential to detect part of its variability (*Birol et al., 2010*). Its large spectrum of variability imposes a very strong constraint on the space-time observation strategy needed to correctly estimate its flow. It turns out that a densification and/or change in the quality of the observations is expected to have a direct impact on the best achievable current estimation. In this work we will not discuss new aspects of the NC but just compare the near-shore surface velocities that can be estimated from X-TRACK/ALES, relative to the ones derived from the AVISO+ X-TRACK 1-Hz SLA.

We focus on Jason track 222 because it crosses the Northern Current over a narrow shelf area, where this continental slope current becomes difficult to observe with altimeter data (*Birol and Delebecque, 2014*). We first spatially filter 20-Hz and 1-Hz Jason SLA by applying a Loess 40-km low-pass filter and then add the mean dynamic topography from *Rio et al. (2014)* to the altimetric SLA in order to obtain the Absolute Dynamic Topography (ADT). Assuming geostrophic balance, the cross-track surface geostrophic velocities have

then been calculated from the along-track ADT gradients (only the velocity component perpendicular to the altimeter pass is reliable from along track altimetric data).

The time-space diagram of the resulting velocity anomalies, computed from both X-TRACK 1 Hz and from X-TRACK/ALES, are in Fig. 6a. Because we focus on the coastal circulation, only the results within 100 km of the coast are shown. We also only consider the 2008-2015 period for clarity reasons. Note that because of its westward direction, the NC corresponds to the negative values observed in the 0-60 km coastal band. In addition, for each altimetry point and each dataset, we also compute the number of velocity estimates available over the period of interest, as well as the corresponding time-average and standard deviation current values. These statistics are represented as a function of the distance to the coast in Figure 6b.

If we first consider the observability of the NC based on X-TRACK 1 Hz (Fig 6a, top and black dataset in Figure 6b), the number of observations decreases abruptly at 20 km to the coast and stops at ~10 km to the coast. As shown in *Biol and Delebecque, 2014*, the NC is captured but not fully resolved. In comparison, if we now consider X/TRACK/ALES current estimations, the amount of data is significantly larger in the 10-20 km coastal band and then stops at ~5 km to the coast. By construction, the number of altimetry points is 20 times larger (e.g. 20-Hz instead of 1-Hz). Even if the spatial filter applied on the SLA data is the same on both datasets before derivation of the current estimates, the resolution is significantly improved in X-TRACK/ALES. As a consequence, the NC is much better resolved than with X-TRACK 1Hz data. Some noisy current estimates remain in the 5-10 km coastal band but the current calculation strategy used here could be further improved (for example by applying an editing procedure).

## **5. Conclusion and perspectives**

During the last decade, several approaches have been proposed to reprocess coastal altimetry measurements from various pulse-limited altimetry missions, leading to great progress in the accuracy and availability of coastal sea level data within 50 km to land (*Benveniste et al.*, 2019). Experimental coastal altimetry products have been validated, showing that the derivation of coastal sea level estimates by altimetry is feasible and highly relevant for many scientific applications. In parallel, recent technologies (the Ka-band of the AltiKa altimeter, the SAR mode adopted in CryoSat-2 and Sentinel-3 missions) allow researchers to further enhance the accuracy and quantity of the near-shore geophysical estimates derived from altimetry but the corresponding sea level record remains relatively short. The challenge today is to obtain the longest sea level time series suitable for coastal sea level studies in the 0–10 km band. This is the objective of the on-going ESA CCI project.

In this study, we have combined the ALES retracking algorithm, the regional X-TRACK processing system and the best possible set of altimetry corrections in order to derive a 16-year-long (June 2002 to May 2018), high-resolution (20-Hz), along-track sea level dataset in six regions (Northeast Atlantic, Mediterranean Sea, West Africa, North Indian Ocean, Southeast Asia and Australia). When comparing available coastal sea level data of the X-TRACK/ALES product to those of X-TRACK 20-Hz and the X-TRACK 1-Hz sea level datasets in the different coastal zones covered by the project, we extend the spatial coverage of the data by getting ~3.5 km closer to the land. We reach a distance of 1.2-4 km to the coast when combining measurements from Jason-1 to Jason-3, with a large increase in the percentage of available coastal sea level data from Jason-1 to Jason-3: on average, we obtain values of 3.6 km, 1.9 km and 0.9 km to the coast, for Jason-1, Jason-2 and Jason-3, respectively. This data gain is also clearly associated to an increase in accuracy of the near-coastal sea level estimates. A comparison with tide gauge observations has been performed at many sites where the Jason tracks cross land in the vicinity of a tide gauge station. The issues

of differences in temporal sampling and location of the data have been alleviated by selecting altimetry data based on the characteristic length scales of the sea-level signal around the tide gauges, allowing a more proper assessment of the altimetry data. We have found that the new X-TRACK/ALES coastal sea-level product provides a very good agreement with tide gauge observations in terms of correlations (average of 0.77) and of value of the annual cycle (differences of 17% in terms of amplitude). We have then shown that, from this dataset, it is possible to derive an estimation of the ocean current variability up to 5 km to the coast.

The validated X-TRACK/ALES coastal sea-level product presented in this study is freely available to users. In the context of the on-going ESA CCI project, we plan now to extend the corresponding dataset in time and space, both by updating the Jason-3 record and by including additional altimeter missions (Envisat, SARAL/Altika, Sentinel-3A, Sentinel-3B). We will also add other regions in the study, in particular the whole African coasts and the coasts of North and South America. Future activities will also be devoted to investigate the altimetry corrections and aspects of the sea level data processing that most limit the availability and accuracy of the sea level variability derived from the product, and then the interpretation of near-shore oceanographic signals. It will be made using in situ data and/or high-resolution hydrodynamical models where available.

Finally, the availability of this new product should help answering questions related to the coastal sea level variability and changes. It will provide a valuable contribution to altimetry in coastal marine research community

### **Acknowledgements:**

This work was funded by the European Space Agency during the two phases of the Climate Change Initiative (CCI) for Sea Level and the CCI+ phase for Coastal Sea Level and the French Ministry of Research. Support from these institutions is gratefully acknowledged. The

X-TRACK altimetry data used in this study were developed, validated, and distributed by AVISO+, <https://www.aviso.altimetry.fr/index.php?id=3047>). We wish also to acknowledge the contribution of the services that make the tide gauge data available: SHOM (<https://data.shom.fr>), the University of Hawaii (<http://uhslc.soest.hawaii.edu/network/>) and Permanent Service for Mean Sea Level (<http://www.psmsl.org/>). Finally, we also thank the two anonymous reviewers for their comments that helped to improve the manuscript.

## References

Ablain, M., Cazenave A., Larnicol G., Balmaseda M., Cipollini P., Faugère Y., Fernandes M.J., Henry O., Johannessen J.A., Knudsen P., Andersen O., Legeais J.F., Meyssignac B., Picot N., Roca M., Rudenko S., Scharffenberg M.G., Stammer D., Timms G., Benveniste J., 2015. Improved sea level record over the satellite altimetry era (1993–2010) from the Climate Change Initiative Project. *Ocean Sci.*, 11, 67-82, doi:10.5194/os-11-67-2015.

Ablain, M., Legeais, J.F., Prandi, P., Fenoglio-Marc L., Marcos M., Benveniste J., Cazenave A., 2017. Satellite Altimetry-Based Sea Level at Global and regional Scales, *Surv Geophys.* 38: 7. doi:10.1007/s10712-016-9389-8.

Andersen, O. B., Scharroo, R., 2011. Range and geophysical corrections in coastal regions: and implications for mean sea surface determination. In *Coastal Altimetry* (eds. Vignudelli, S., Kostianoy, A., Cipollini, P., and J Benveniste, J.). Springer, Berlin Heidelberg, 103-146, doi:10.1007/978-3-642-12796-0\_5.

Benveniste J., Cazenave A., Vignudelli S., Fenoglio-Marc L., Shah R., Almar R., Andersen O., Birol F., Bonnefond P., Bouffard J., Calafat F., Cardellach E., Cipollini P., Le Cozannet G., Dufau C., Fernandes M.J., Frappart F., Garrison J., Gommenginger C., Han G., Høyer J.L., Kourafalou V., Leuliette E., Li Z., Loisel H., Madsen K.S., Marcos M., Melet A., Meyssignac B., Pascual A., Passaro M., Ribó S., Scharroo R., Song Y.T., Speich S., Wilkin J., Woodworth P., Wöppelmann G., 2019. Requirements for a Coastal Hazards Observing System. *Frontiers in Marine Science*, vol. 6 p.348, <https://www.frontiersin.org/article/10.3389/fmars.2019.00348>.

Birol F., M. Cancet M., Estournel C., 2010. Aspects of the seasonal variability of the Northern Current (NW Mediterranean Sea) observed by altimetry. *J. of Mar. Systems*, doi:10.1016/j.jmarsys.2010.01.005.

Birol F., Delebecque C., 2014. Using high sampling rate (10/20 Hz) altimeter data for the observation of coastal surface currents: A case study over the northwestern Mediterranean Sea, *J. Mar. Syst.*, doi:10.1016/j.jmarsys.2013.07.009.

Birol F., Niño F., 2015. Ku and Ka-band altimeter data in the northwestern Mediterranean Sea. *SARAL/Altika Special Issue* 38. <http://dx.doi.org/10.1080/01490419.2015.1034814>.

Birol F., Fuller, N., Lyard, F., Cancet, M., Niño, F., Delebecque, C., Fleury, S., Toubanc, F., Melet, A., Saraceno, M., Léger, F., 2017. Coastal applications from nadir altimetry: Example of the X-TRACK regional products. *Advances in Space Research* 59, 936–953. <https://doi.org/10.1016/j.asr.2016.11.005>.

Carrere L., Lyard, F., 2003. Modeling the barotropic response of the global ocean to atmospheric wind and pressure forcing-Comparisons with observations. *Geophys. Res. Lett.*, 30(6), 1275, <https://doi.org/10.1029/2002GL016473>.

Carrere L., Lyard, F., Cancet, M., Guillot, A., Roblou, L., 2012. FES2012: A new global tidal model taking advantage of nearly 20 years of altimetry, in *Proceedings of the “20 Years of Progress in Radar Altimetry” Symposium, Venice, Italy, 24-29 September 2012, ESA Special Publication SP-710, 2012.*

Carrere L., F. Lyard, M. Cancet, A. Guillot, N. Picot, 2016. FES 2014, a new tidal model – Validation results and perspectives for improvements, presentation to *ESA Living Planet Conference, Prague.*

Carret A., Birol, F., Estournel, C., Zakardjian, B., Testor, P., 2019. Synergy between in situ and altimetry data to observe and study the Northern Current variations (NW Mediterranean Sea), *Ocean Sci. Discuss., Ocean Sci.*, 15, 269-290, <https://doi.org/10.5194/os-15-269-2019>.

Cartwright, D.E., Tayler R.J., 1971. New computations of the tide-generating potential. *Geophys. J. Int.*, 23, pp. 45-73, <https://doi.org/10.1111/j.1365-246X.1971.tb01803.x>.

Cartwright, D.E., Edden A.C., 1973. Corrected table of tidal harmonics, *Geophys. J. R. Astron. Soc.*, 33, 253–264, <https://doi.org/10.1111/j.1365-246X.1973.tb03420.x>.

Cipollini, P., Calafat, F.M., Jevrejeva, S., Melet, A., Prandi, P., 2017. Monitoring Sea Level in the Coastal Zone with Satellite Altimetry and Tide Gauges. *Surveys in Geophysics*. <https://doi.org/10.1007/s10712-016-9392-0>.

Desjonquères, J.D., Carayon, G., Steunou, N., Lambin, J., 2010. Poseidon-3 radar altimeter: new modes and in-flight performances. *Mar. Geod.* 34. <https://dx.doi.org/10.1080/01490419.2010.488970>.

Dinardo S, Fenoglio-Marc L, Buchhaupt C, Becker M, Scharroo R, Fernandes MJ, Benveniste J, 2018. Coastal SAR and PLRM altimetry in German Bight and West Baltic Sea. *Adv Space Res* 62(6):1371–1404. <https://doi.org/10.1016/j.asr.2017.12.018>.

Fernandes M.J., C. Lázaro, M. Ablain, Pires N., 2015. Improved wet path delays for all ESA and reference altimetric missions, *Remote Sensing of Environment*, Volume 169, November 2015, Pages 50-74, ISSN 0034-4257, <http://dx.doi.org/10.1016/j.rse.2015.07.023>.

Fernandes, M., Lázaro C., 2016. GPD+ Wet Tropospheric Corrections for CryoSat-2 and GFO Altimetry Missions. *Remote Sensing* 8 (10): 851. doi:10.3390/rs8100851.

Gómez-Enri J, González CJ, Passaro M, Vignudelli S, Álvarez O, Cipollini P, Mañanes R, Bruno M, Lopez-Carmona P, Izquierdo A, 2019. Wind-induced cross-strait sea level variability in the Strait of Gibraltar using coastal altimetry and in-situ measurements. *Remote Sens Environ* 221:596–608. <https://doi.org/10.1016/j.rse.2018.11.042>.

Gommenginger, C., Thibaut, P., Fenoglio-Marc, L., Quartly, G., Deng, X., Gómez-Enri, J., Challenor, P., Gao, Y., 2011. Retracking altimeter waveforms near the coasts — a

review of retracking methods and some applications to coastal waveforms. In: Vignudelli, S., Kostianoy, A., Cipollini, P., Benveniste, J. (Eds.), Coastal Altimetry. Springer, [https://doi.org/10.1007/978-3-642-12796-0\\_4](https://doi.org/10.1007/978-3-642-12796-0_4).

Gouzenes Y., Léger, F., Cazenave, A., Birol, F., Bonnefond, P., Passaro, M., Nino, F., Almar, R., Laurain, O., Schwatke, C., Legeais, J.-F., Benveniste, J., 2020. Coastal Sea Level rise at Senetosa (Corsica) during the Jason altimetry missions, *Ocean Science*, os-2020-3. <https://doi.org/10.5194/os-16-1165-2020>.

Holgate, S.J.; Matthews, A.; Woodworth, P.L.; Rickards, L.J.; Tamisiea, M.E.; Bradshaw, E.; Foden, P.R.; Gordon, K.M.; Jevrejeva, S., Pugh, J., 2013. New data systems and products at the Permanent Service for Mean Sea Level. *Journal of Coastal Research*, 29 (3). 493-504. <https://doi.org/10.2112/JCOASTRES-D-12-00175.1>.

Jebri, F., Birol, F., Zakardjian, B., Bouffard, J., Sammari, C., 2016. Exploiting coastal altimetry to improve the surface circulation scheme over the central Mediterranean Sea. *Journal of Geophysical Research: Oceans*. <https://doi.org/10.1002/2016JC011961>.

Legeais, J.-F., Ablain, M., Zawadzki, L., Zuo, H., Johannessen, J. A., Scharffenberg, M. G., Fenoglio-Marc, L., Fernandes, M. J., Andersen, O. B., Rudenko, S., Cipollini, P., Quartly, G. D., Passaro, M., Cazenave, A., Benveniste, J., 2018. An improved and homogeneous altimeter sea level record from the ESA Climate Change Initiative, *Earth Syst. Sci. Data*, 10, 281-301, <https://doi.org/10.5194/essd-10-281-2018>.

Marcos M., Rohmer J., Vousedoukas M.I., Mentaschi L., Le Cozannet L., et al., 2019. Increased Extreme Coastal Water Levels Due to the Combined Action of Storm Surges and Wind Waves. *Geophysical Research Letters*, 46 (8), pp.4356-4364.

Marti, F., Cazenave, A., Birol, F., Passaro, M., Leger, F., Nino, F., Almar, R., Benveniste, J., Legeais, J.F., 2019. Altimetry-based sea level trends along the coasts of western Africa. *Advances in Space Research*. <https://doi.org/10.1016/j.asr.2019.05.033>.

Mercier F., Rosmorduc, V., Carrere, L., Thibaut, P., 2010. Coastal and Hydrology Altimetry Product (PISTACH) Handbook; CLS-DOS-NT-10-246; CNES: Paris, France.

Millot C., 1991. Mesoscale and seasonal variabilities of the circulation in the western Mediterranean. *Dyn. Atmos. Oceans* 15, 179-214.

Passaro M., Cipollini P., Vignudelli S., Quartly G., Snaith H., 2014. ALES: A multi-mission subwaveform retracker for coastal and open ocean altimetry. *Remote Sensing of Environment* 145, 173-189, doi:10.1016/j.rse.2014.02.008.

Passaro M., Cipollini P., Benveniste J., 2015. Annual sea level variability of the coastal ocean: The Baltic Sea-North Sea transition zone. *Journal of Geophysical Research* 120(4): 3061-3078, doi:10.1002/2014JC010510.

Passaro M., Zulfikar Adlan N., Quartly G.D, 2018. Improving the precision of sea level data from satellite altimetry with high-frequency and regional sea state bias corrections. *Remote Sensing of Environment*, 245-254, doi:10.1016/j.rse.2018.09.007.

Peng, F.K., Deng, X.L., 2018. A new retracking technique for Brown peaky altimetric waveforms. *Marine Geodesy*, 41(2), 99-125, <https://doi.org/10.1080/01490419.2017.1381656>.

Piccioni G., Dettmering D., Passaro M., Schwatke C., Bosch W., Seitz F., 2018. Coastal Improvements for Tide Models: The Impact of ALES Retracker. *Remote Sensing*, 10(5), 10.3390/rs10050700.

Quartly, G. D., Legeais, J.-F., Ablain, M., Zawadzki, L., Fernandes, M. J., Rudenko, S., Carrère, L., García, P. N., Cipollini, P., Andersen, O. B., Poisson, J.-C., Mbajon Njiche, S., Cazenave, A., Benveniste, J., 2017. A new phase in the production of quality-controlled sea level data, *Earth Syst. Sci. Data*, 9, 557–572, <https://doi.org/10.5194/essd-9-557-2017>.

Rasmussen C.E., Williams C. K. I., 2006. *Gaussian Processes for Machine Learning*, the MIT Press, ISBN 026218253X.

Rio, M.-H., Pascual, A., Poulain, P.-M., Menna, M., Barceló, B., Tintoré, J., 2014. Computation of a new mean dynamic topography for the Mediterranean Sea from model outputs, altimeter measurements and oceanographic in situ data, *Ocean Sci.*, 10, 731–744, <https://doi.org/10.5194/os-10-731-2014>.

Roblou, L., Lamouroux, J., Bouffard, J., Lyard, F., Le Hénaff, M., Lombard, A., Marsalaix, P., De Mey, P., Birol, F., 2011. Post-processing altimeter data toward coastal applications and integration into coastal models. Chapter 9. In: Vignudelli, S., Kostianoy, A.G., Cipollini, P., Benveniste, J. (Eds.), *Coastal Altimetry*. Springer Berlin Heidelberg, [https://doi.org/10.1007/978-3-642-12796-0\\_9](https://doi.org/10.1007/978-3-642-12796-0_9).

Smith W.H.F., Leuliette E.W., Passaro M., Quartly G., Cipollini P.: Covariant errors in ocean retracers evaluated using along-track cross-spectra. OSTST Meeting 2017, Miami, USA, 2017.

The Climate Change Coastal Sea Level team, Benveniste, J., Birol, F. *et al.* 2020. Coastal sea level anomalies and associated trends from Jason satellite altimetry over 2002-2018. *Sci. Data (Nature)*, 7, 357, <https://doi.org/10.1038/s41597-020-00694-w>.

Tran, N., Labroue, S., Philipps, S., Bronner, E., Picot, N., 2010. Overview and Update of the Sea State Bias Corrections for the Jason-2, Jason-1 and TOPEX Missions. *Marine Geodesy*, 33, 348, doi:10.1080/01490419.2010.487788.

Troupin, C., Pascual, A., Valladeau, G., Pujol, I., Lana, A., Heslop, E., Ruiz, S., Torner, M., Picot, N., Tintoré, J., 2015. Illustration of the emerging capabilities of SARAL/AltiKa in the coastal zone using a multi-platform approach. *Advances in Space Research*, 55 (1), 51-59, doi:10.1016/j.asr.2014.09.011.

Valladeau V., Thibaut P., Picard B., Poisson J.C., Tran N., Picot N. Guillot A., 2015. Using SARAL/AltiKa to Improve Ka-band Altimeter Measurements for Coastal Zones,

Hydrology and Ice: The PEACHI Prototype. *Marine Geodesy*, 38:sup1, 124-142, doi: 10.1080/01490419.2015.1020176.

Verron, J., Bonnefond, P., Aouf, L., Birol, F., Bhowmick, S.A., Calmant, S., Conchy, T., Crétaux, J.-F., Dibarboure, G., Dubey, A.K., Faugère, Y., Guerreiro, K., Gupta, P.K., Hamon, M., Jebri, F., Kumar, R., Morrow, R., Pascual, A., Pujol, M.-I., Rémy, E., Rémy, F., Smith, W.H.F., Tournadre, J., Vergara, O., 2018. The Benefits of the Ka-Band as Evidenced from the SARAL/AltiKa Altimetric Mission: Scientific Applications. *Remote Sensing*, 10, 163, doi: 10.3390/rs10020163.

Vignudelli, S., Cipollini, P., Roblou, L., Lyard, F., Gasparini, G. P., Manzella, G., Astraldi, M., 2005. Improved satellite altimetry in coastal systems: Case study of the Corsica Channel (Mediterranean Sea), *Geophysical Research Letters*, 32, L07608, doi:10.1029/2005GL022602.

Vignudelli, S. *et al.*, 2009. The COASTALT project: Towards an operational use of satellite altimetry in the coastal zone. *OCEANS 2009*, Biloxi, MS, pp. 1-6, doi: 10.23919/OCEANS.2009.5422467.

Vignudelli, S., Kostianoy, A.G., P. Cipollini, P., Benveniste J. (Eds.), 2011. *Coastal Altimetry*, Springer, Berlin Heidelberg, 578 pp, doi:10.1007/978-3-642-12796-0.

Vignudelli S., F. Birol, J. Benveniste, L.-L. Fu, N. Picot, M. Raynal, H. Roinard, 2019. Satellite altimetry measurements of sea level in the coastal zone. *Surveys in Geophysics*. DOI 10.1007/s10712-019-09569-1.

Wahr, J. M., 1985. Deformation induced by polar motion, *J. Geophys. Res.*, 90(B11), 9363– 9368.

Xu X., F. Birol, Cazenave A., 2018. Evaluation of coastal sea level of Jason-2 altimetry offshore Hong Kong, *Remote Sensing*, 25. 10.3390/rs10020282.

**Tables:**

| Parameter              | source              | Jason-1 / Jason-2 / Jason-3                                                                 |
|------------------------|---------------------|---------------------------------------------------------------------------------------------|
| Altitude               | GDR                 | Altitude of satellite                                                                       |
| Range                  | ALES/TUM            | 20 Hz ku band ALES corrected altimeter range ( <i>Passaro et al., 2014</i> )                |
| Ionosphere             | GDR                 | From dual-frequency altimeter range measurement                                             |
| Dry troposphere        | GDR                 | From ECMWF model                                                                            |
| Wet troposphere        | University of Porto | GPD+ radiometer correction ( <i>Fernandes et al. 2015</i> )                                 |
| Sea state bias         | ALES/TUM            | Sea state bias correction in ku band, ALES retracking ( <i>Passaro et al., 2018</i> )       |
| Solid tides            | RADS                | From tide potential model ( <i>Cartwright and Taylor, 1971, Cartwright and Eden, 1973</i> ) |
| Pole tides             | GDR                 | From <i>Wahr, 1985</i>                                                                      |
| Loading effect         | RADS                | From FES 2014 ( <i>Carrere et al., 2012</i> )                                               |
| Atmospheric correction | RADS                | From MOG2D-G ( <i>Carrere and Lyard, 2003</i> ) + inverse barometer                         |
| Ocean tide             | RADS                | From FES 2014 ( <i>Carrere et al., 2016</i> )                                               |

**Table 1: List of altimetry parameters and geophysical corrections used in the computation of X-TRACK/ALES coastal sea level product.**

| Region              | Mission | Number of tracks | Dataset     |              |              |
|---------------------|---------|------------------|-------------|--------------|--------------|
|                     |         |                  | X-TRACK 1Hz | X-TRACK 20Hz | X-TRACK/ALES |
| Mediterranean Sea   | Jason-1 | 30               | 6.9         | 4.2          | 3.31         |
|                     | Jason-2 |                  | 5.25        | 1.44         | 1.19         |
| Northern Europe     | Jason-1 | 27               | 6.23        | 4.12         | 3.94         |
|                     | Jason-2 |                  | 5.83        | 1.94         | 1.94         |
| Western Africa      | Jason-1 | 24               | 9.26        | 6.05         | 4.84         |
|                     | Jason-2 |                  | 7.56        | 4.54         | 3.38         |
| Mean over 3 regions | Jason-1 | 81               | 7.46        | 4.79         | 4.03         |
|                     | Jason-2 |                  | 6.21        | 2.64         | 2.39         |

**Table 2: Median distance to the coast of the first point (in km) where more than 80% of the SLA data are available in the time series, for both Jason1 and Jason2, for each region, and average value obtained for the three regions (see Fig. 2). The number of tracks used to compute the statistics is also indicated. Note that in each region, only tracks crossing land have been considered.**

| Region              | Name of TG / Jason track number | Statistics                            | X-TRACK 1 Hz |          | X-TRACK 20 Hz |          | X-TRACK/ALES |          |
|---------------------|---------------------------------|---------------------------------------|--------------|----------|---------------|----------|--------------|----------|
|                     |                                 |                                       | raw          | filtered | raw           | filtered | raw          | filtered |
| West Africa         | Sao Tome<br>Track 033           | Distance altimetry vs TG data (in km) | 25.08        |          | 24.37         |          | 24.37        |          |
|                     |                                 | Number of data available              | 171          |          | 141           |          | 156          |          |
|                     |                                 | Correlation                           | 0.49         | 0.63     | 0.31          | 0.54     | 0.39         | 0.68     |
|                     |                                 | RMSD (m)                              | 0.080        | 0.067    | 0.147         | 0.075    | 0.111        | 0.063    |
|                     | Dakar<br>Track 174              | Distance altimetry vs TG data (in km) | 9.41         |          | 4.26          |          | 3.91         |          |
|                     |                                 | Number of data available              | 320          |          | 258           |          | 294          |          |
|                     |                                 | Correlation                           | 0.89         | 0.91     | 0.38          | 0.91     | 0.40         | 0.92     |
|                     |                                 | RMSD (m)                              | 0.039        | 0.035    | 0.152         | 0.035    | 0.137        | 0.033    |
| North East Atlantic | St Jean de Luz<br>Track 248     | Distance altimetry vs TG data (in km) | 15.34        |          | 8.86          |          | 8.36         |          |
|                     |                                 | Number of data available              | 341          |          | 296           |          | 301          |          |
|                     |                                 | Correlation                           | 0.72         | 0.74     | 0.20          | 0.75     | 0.28         | 0.79     |
|                     |                                 | RMSD (m)                              | 0.060        | 0.052    | 0.222         | 0.053    | 0.137        | 0.047    |
|                     | Roscoff<br>Track 070            | Distance altimetry vs TG data (in km) | 9.66         |          | 8.91          |          | 8.34         |          |
|                     |                                 | Number of data available              | 370          |          | 349           |          | 397          |          |
|                     |                                 | Correlation                           | 0.49         | 0.59     | 0.26          | 0.63     | 0.40         | 0.68     |
|                     |                                 | RMSD (m)                              | 0.149        | 0.105    | 0.234         | 0.089    | 0.157        | 0.076    |
|                     | Senetosa<br>Track 085           | Distance altimetry vs TG data (in km) | 9.69         |          | 4.93          |          | 4.93         |          |
|                     |                                 | Number of data available              | 416          |          | 359           |          | 367          |          |
|                     |                                 | Correlation                           | 0.77         | 0.88     | 0.56          | 0.84     | 0.60         | 0.90     |
|                     |                                 | RMSD (m)                              | 0.053        | 0.033    | 0.107         | 0.042    | 0.096        | 0.032    |
| Mediterranean Sea   | Sète<br>Track 146               | Distance altimetry vs TG data (in km) | 18.08        |          | 15.65         |          | 15.57        |          |
|                     |                                 | Number of data available              | 362          |          | 326           |          | 349          |          |
|                     |                                 | Correlation                           | 0.77         | 0.82     | 0.56          | 0.79     | 0.55         | 0.79     |
|                     |                                 | RMSD (m)                              | 0.059        | 0.055    | 0.122         | 0.059    | 0.112        | 0.055    |

**Table 3: RMSD (in meters) and correlation coefficients obtained from the comparison of altimetry and tide gauge (TG) coincident SLA time series. Statistics are given for X-TRACK, X-TRACK/20Hz and X-TRACK/ALES, for both raw and Loess low-pass filtered SLA. The distance (in km) between the altimetry and tide gauge observations is also provided, as well as the number of samples available to compute the statistics.**

| Region                | Mission |         |         |                      |
|-----------------------|---------|---------|---------|----------------------|
|                       | Jason-1 | Jason-2 | Jason-3 | Combined Jason-1,2,3 |
| Mediterranean Sea     | 3.3     | 1.2     | 0.6     | 1.9                  |
| Northern Europe       | 3.9     | 1.9     | 1.1     | 3.2                  |
| Western Africa        | 4.7     | 3.4     | 1.3     | 4.0                  |
| North Indian Ocean    | 4.5     | 2.9     | 1.2     | 3.8                  |
| Southeast Asia        | 1.7     | 1.0     | 0.5     | 1.2                  |
| Australia             | 3.7     | 1.1     | 0.9     | 3.4                  |
| MEAN OVER ALL REGIONS | 3.6     | 1.9     | 0.9     | 2.9                  |

**Table 4: Median distance to the coast of the first altimetry point (in km) where more than 80% of the SLA data are available in the X-TRACK/ALES time series as a function of the altimeter mission and the region considered. Average values are also computed over the six regions of the SL\_cci+ project for each mission.**

## Figure captions:

**Figure 1:** Bottom middle and right: Time-space diagram of SLA (in meters and as a function of cycles and latitude) along Jason 2 track 9 in the Mediterranean Sea (see top figure) before and after the X-TRACK procedure, respectively. Bottom left: Standard deviation of the corresponding SLA time series (in meters) before (in red) and after (in blue) the X-TRACK procedure.

**Figure 2:** The six regions (red polygons) where the new coastal sea level product has been reprocessed with the X-TRACK/ALES system. The number of Jason tracks for each region is: 32, 30, 35, 42, 55 and 50 for, respectively, Northern Europe, Mediterranean Sea, Western Africa, North Indian Ocean, Southeast Asia and Australia.

**Figure 3:** Boxplot of the distribution of the distance to the coast (in km) of the first altimetry points where the percentage of defined data in the time series is larger than 80% as a function of the region considered. Results are shown for Jason-1 (top) and Jason-2 (bottom), for the standard X-TRACK product (XT 1Hz), X-TRACK 20Hz (XT 20Hz) and X-TRACK/ALES (XT/AL 20Hz). For each region/mission/dataset, all the altimetry tracks available are considered in the statistics. Red lines represent the median values. The bottom and top of the blue rectangles represent, the first and third quartiles, respectively and the black lines the range between minimum and maximum values in the statistics.

**Figure 4:** a) Regional average values of STD deviations (in meters) of the X-TRACK 1-Hz (in black), X-TRACK 20-Hz (in red) and X-TRACK/ALES (in green) Jason-1 SLA as a function of distance to the coast for the 3 regions considered. b) Same for Jason-2.

**Figure 5:** Correlation of detrended, deseasoned sea level from tide gauge records and satellite altimetry (the ‘best’ altimetric timeseries) in (A) the Northeast Atlantic Ocean, (B) the Mediterranean Sea, (C) the Western African coast, (D) the North Indian Ocean, (E) Southeast Asian, and (F) Australia.

**Figure 6:** a) Time space diagram of altimetry-derived currents (in m/s) from X-TRACK 1Hz (top) and X-TRACK/ALES (bottom) for Jason-2 track 222 in the Northwestern Mediterranean Sea. b) Left: Number of altimetry-derived current data as a function of the distance to coast (in km) for X-TRACK 1Hz (black) and X-TRACK/ALES (red) for Jason-2 track 222 in the Northwestern Mediterranean Sea. Right: Corresponding mean current (stars) and standard deviation (lines) values in m/s.

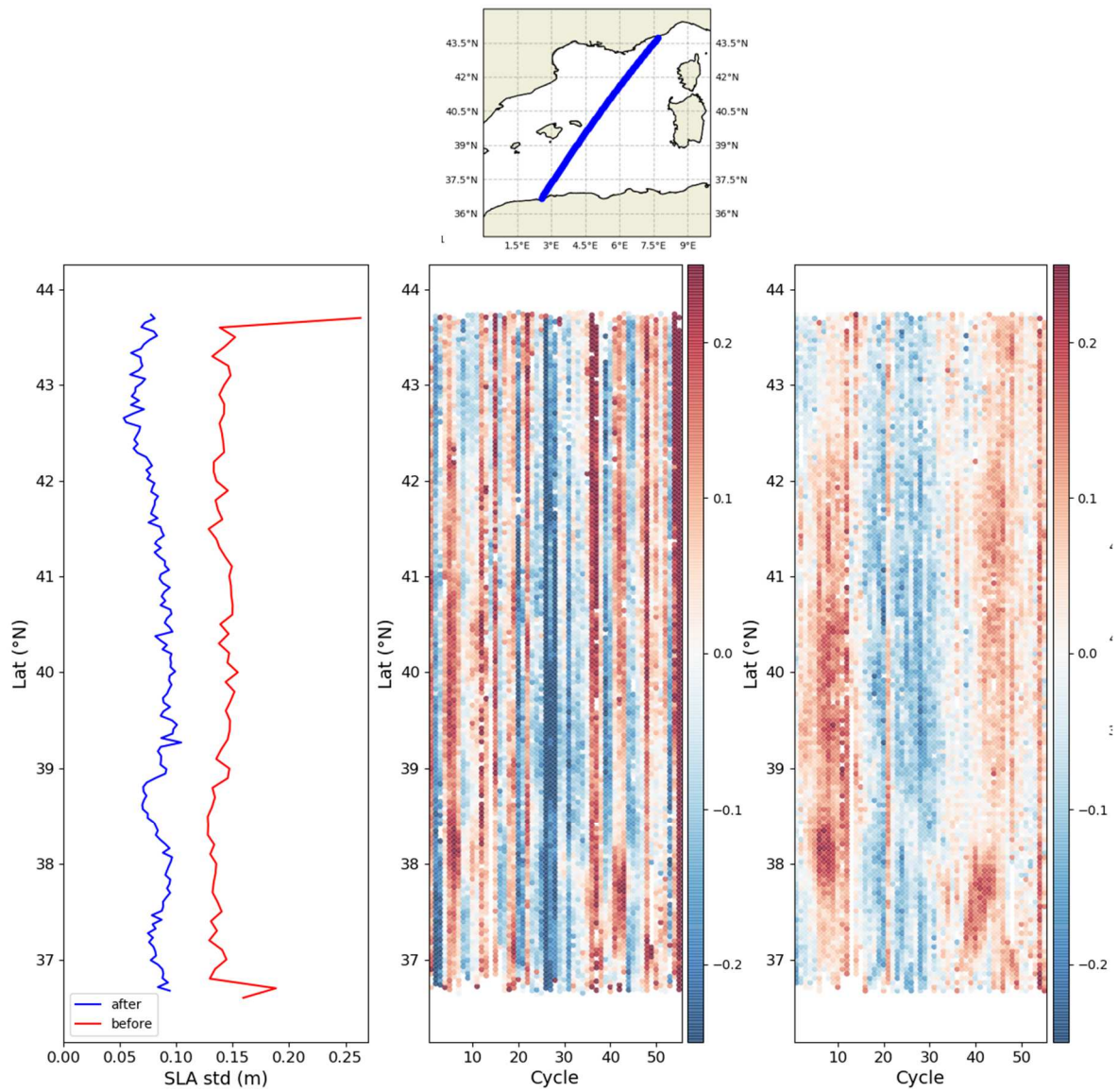


**Figure 1**

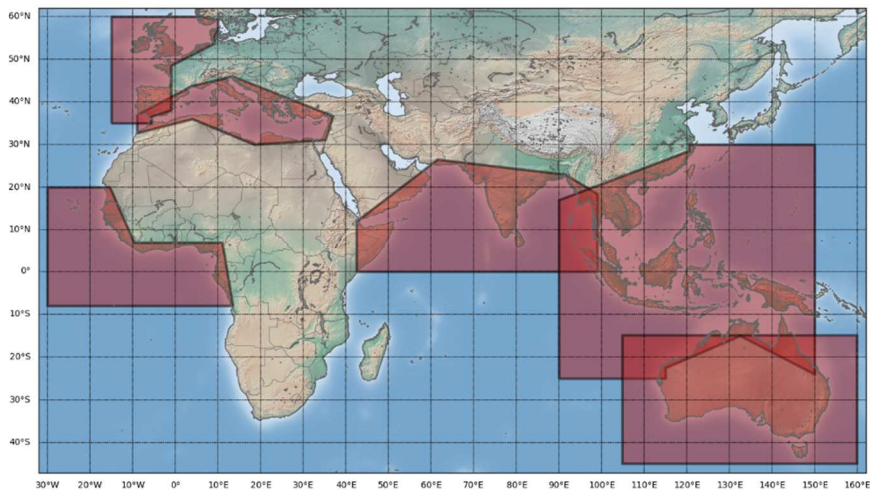


**Figure 2**

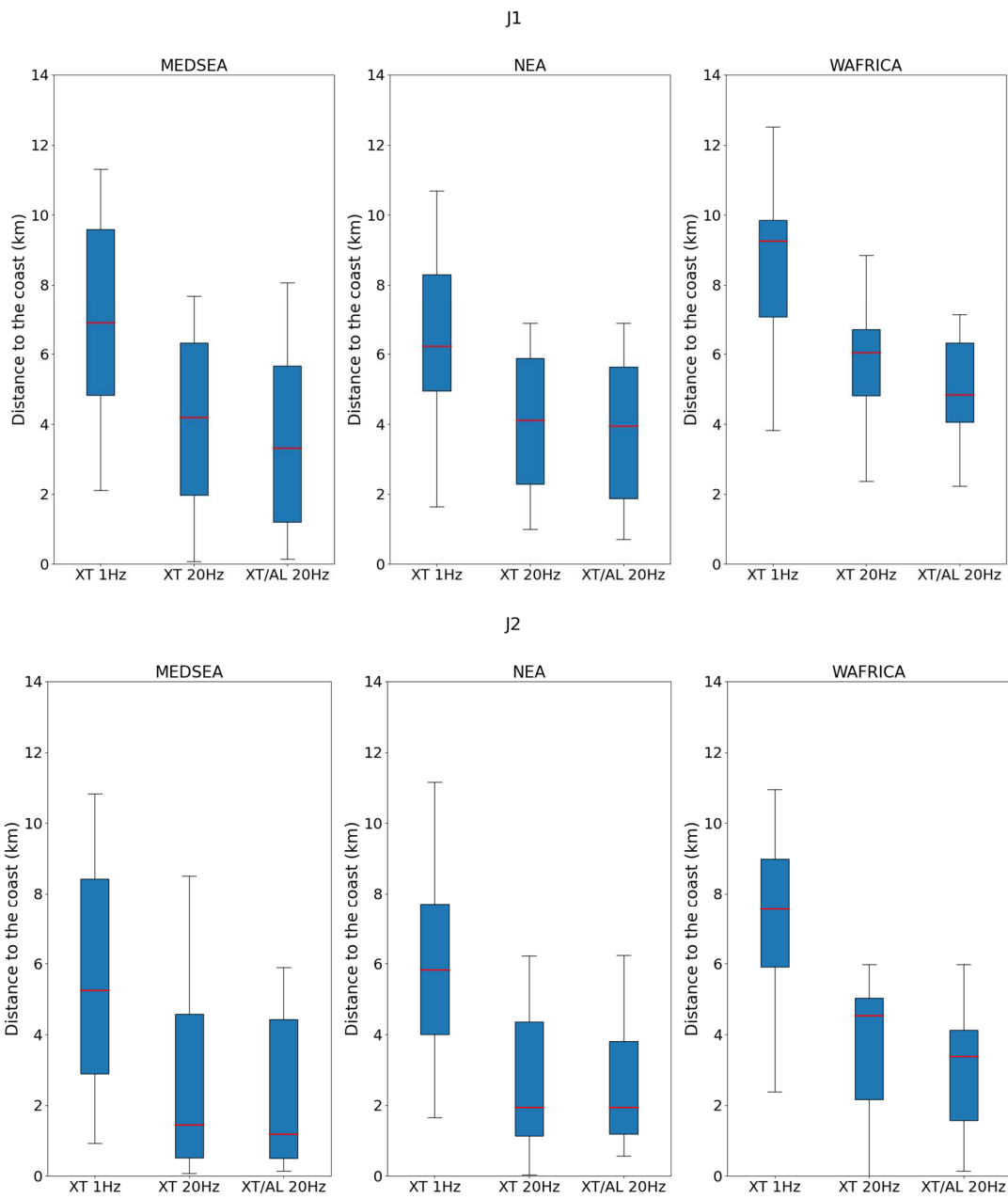


**Figure 3**

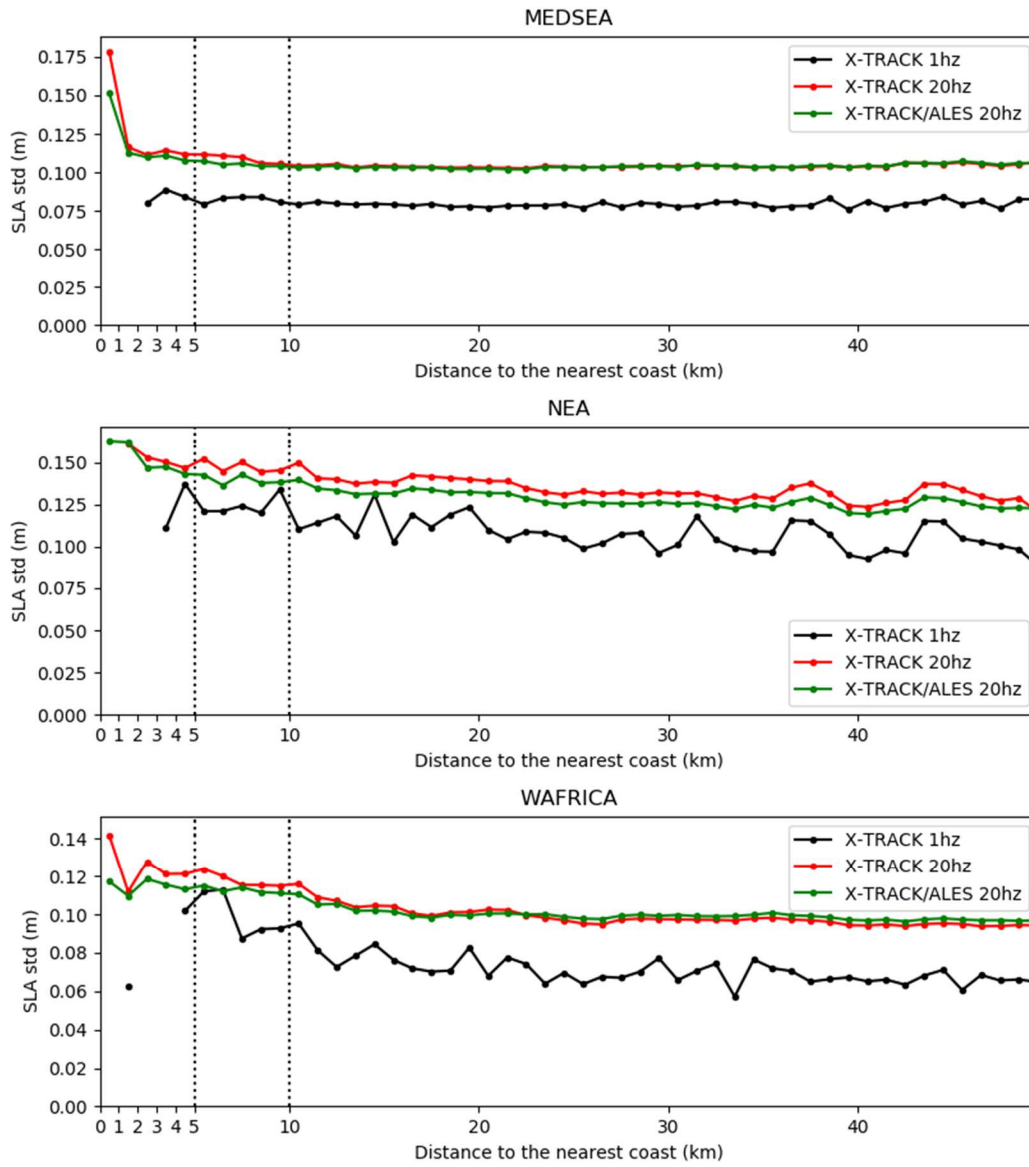


**Figure 4a**

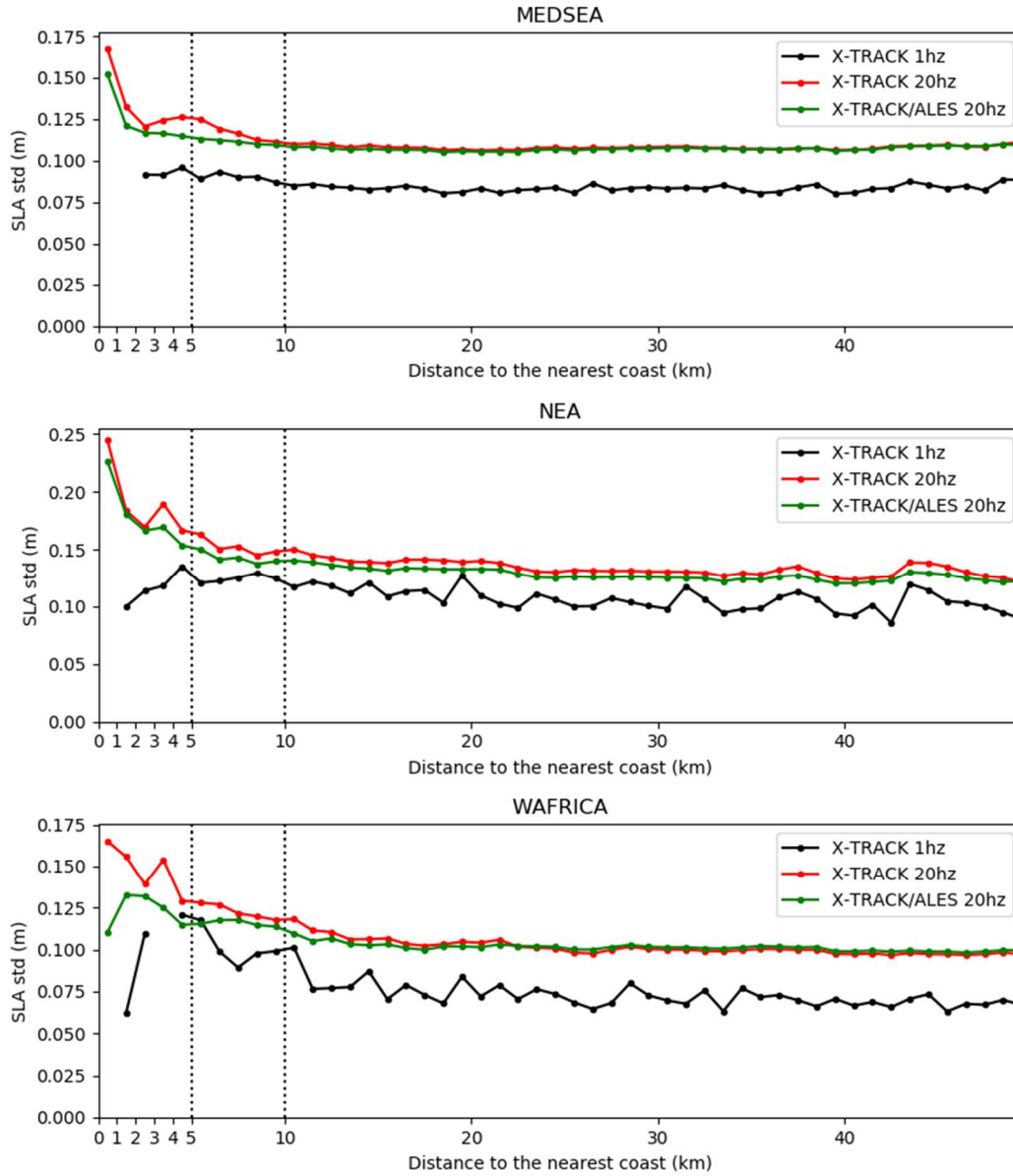


**Figure 4b**

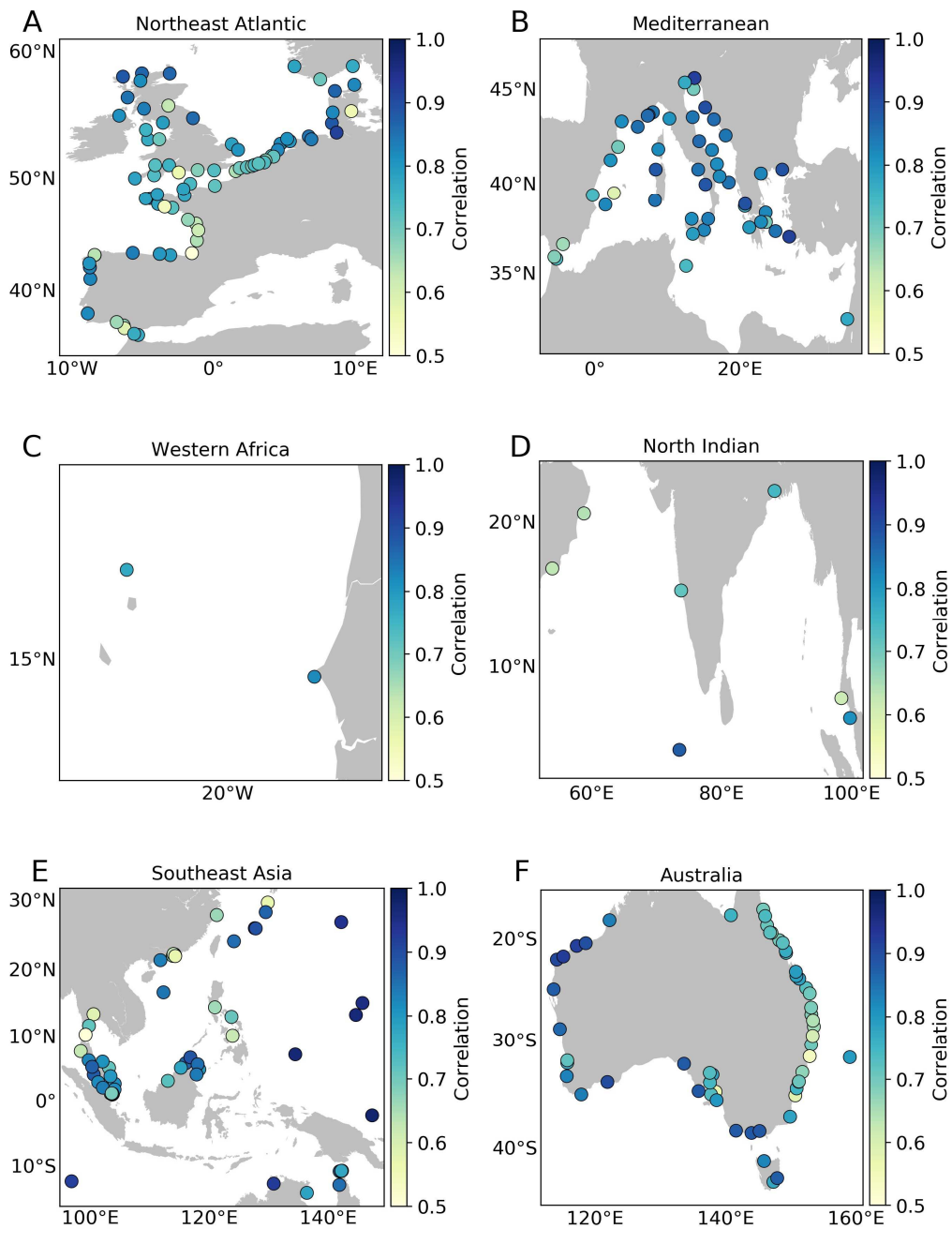


**Figure 5**

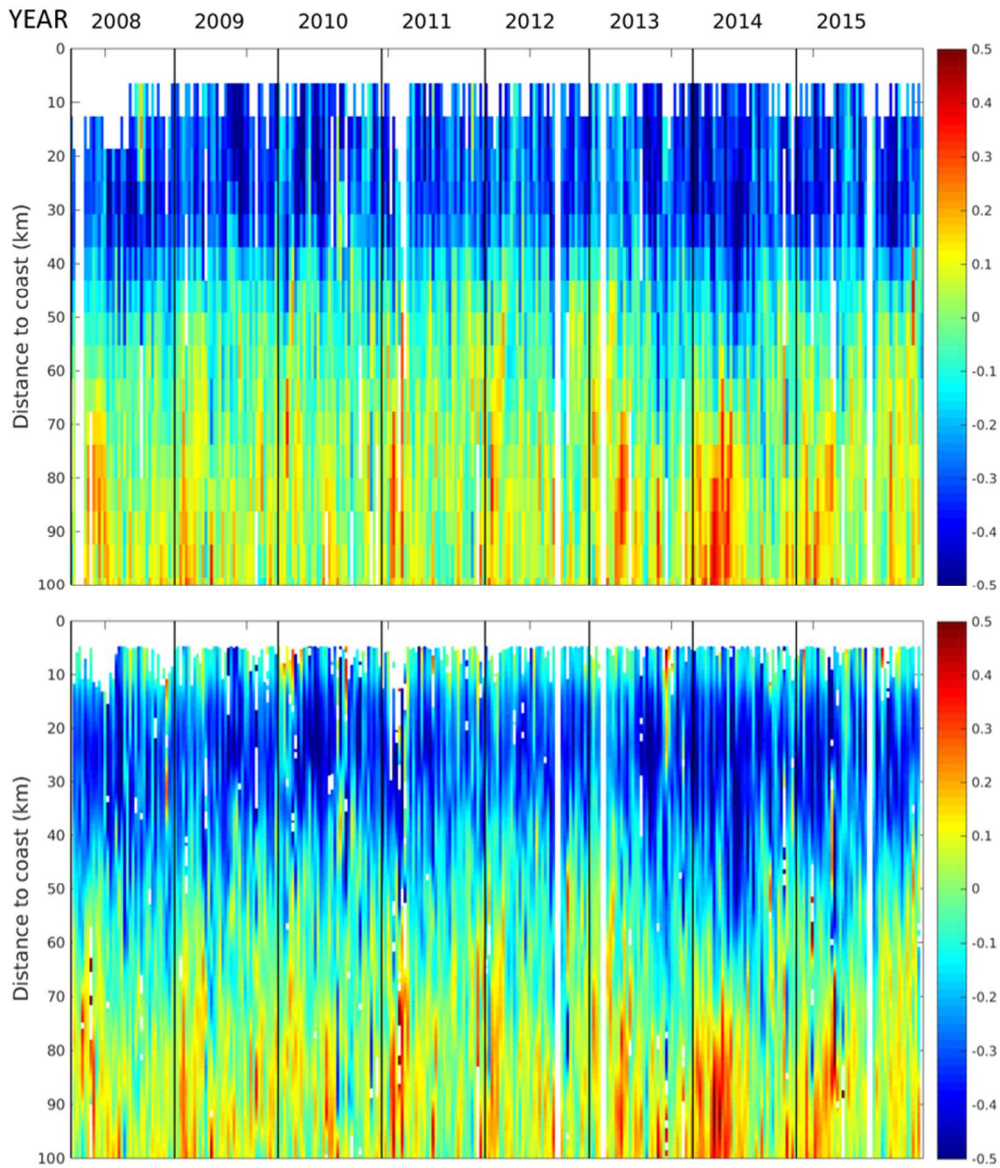


Figure 6a

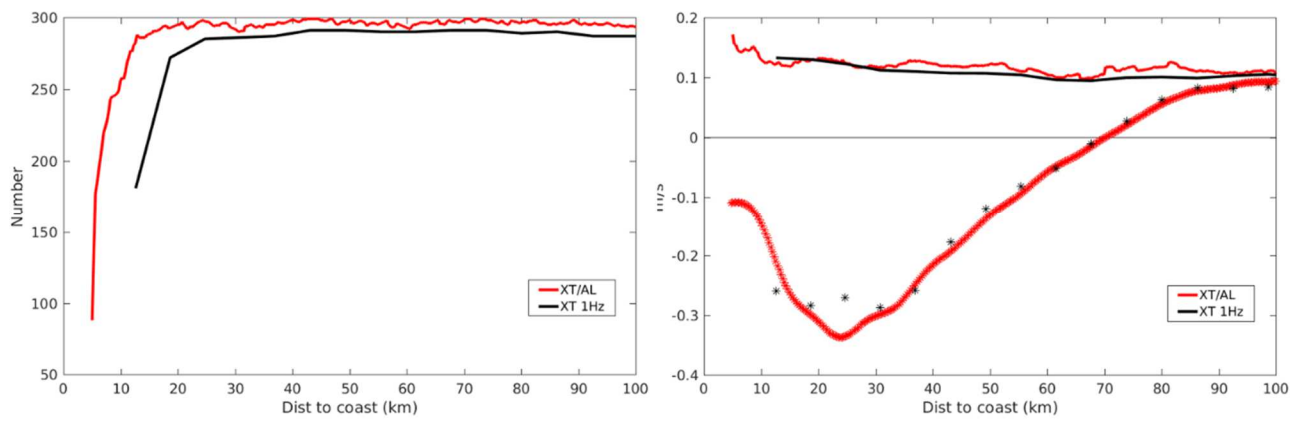


Figure 6b